Supporting Information

For

Experimental and Computational Investigation of the Bond Energy of Thorium Dicarbonyl Cation and Theoretical Elucidation of Its Isomerization Mechanism to the Thermodynamically Most Stable Isomer, Thorium Oxide Ketenylidene Cation, OTh^+CCO

Arjun Kafle and P. B. Armentrout*

Department of Chemistry, University of Utah, 315 S 1400 E Rm 2020, Salt Lake City, UT 84112

Table S1. Molecular parameters calculated at the B3LYP/cc-pVQZ level used for modelling with Eq. (1)

Species (state)	Vibrational frequencies ω_e (cm^{-1})[a]	Rotational constants (B, cm^{-1})
CO ($^1\Sigma^+$)	2214	1.947
$Th^+(CO)$ ($^4\Sigma^-$)	308(2)	0.075
	346	
	1953	
$Th^+(CO)_2$ ($^4B_2$)	43	0.035
	283	0.064
	293	0.078
	294	
	296	
	308	
	349	
	1972	
	2031	

[a] Degeneracies in parentheses

Table S2. Comparison of molecular parameters of ground state of neutral $Th(CO)_2$ (C_{2V}) and OThCCO (C_s) calculated at the B3LYP/cc-pVQZ level compared to the literature

Species	State	Method	r (Å)				∠CThC (°)	∠OThC (°)	C-O stretch ω_e (cm^{-1})	
			Th-C	C-O	Th-O	C-C			anti.symm.	symm.
$Th(CO)_2$ (C_{2v})	$^1A_1$	B3LYP	2.280	1.168			51		1829	1870
$Th(CO)_2$ (C_{2v})	$^1A_1$	PW91[a]	2.251	1.188			50		1734	1766
$Th(CO)_2$ (C_{2v})	$^1A_1$	Experiment [a]							1775.6	1827.7
OTh^+CCO (C_s)	$^1A'$	B3LYP	2.183	1.175	1.877	1.290		116		2119
	$^1A'$	PW91[a]	2.159	1.186	1.886	1.297		116		2082
		Experiment [a]								2048.6

[a] J. Li, B. E. Bursten, M. Zhou and L. Andrews, *Inorg. Chem.*, 2001, **40**, 5448 − 5460.

Table S3. Natural charges and valence electron configuration of C, O, and Th in low-lying states of $Th^+(CO)_2$ (C_{2V} and $D_{\infty h}$) isomer obtained from an NBO analysis calculated at the B3LYP/cc-pVQZ level. Low-lying states are ordered on the basis of their energy with respect to the $^4B_2$ ground state

Species	State	Charge			Configuration		
		Th	C	O	Th	C	O
$Th^+(CO)_2$ (C_{2v})	$^4B_2$	1.47	0.12	-0.35	$[Rn]7s^{0.14}6d^{2.21}5f^{0.21}$	$[He]2s^{1.37}2p^{2.48}$	$[He]2s^{1.70}2p^{4.62}$
	$^4B_1$	1.30	0.20	-0.34	$[Rn]7s^{0.67}6d^{1.81}5f^{0.22}$	$[He]2s^{1.37}2p^{2.40}$	$[He]2s^{1.70}2p^{4.61}$
	$^2B_1$	1.46	0.13	-0.36	$[Rn]7s^{0.63}6d^{1.76}5f^{0.19}$	$[He]2s^{1.33}2p^{2.50}$	$[He]2s^{1.69}2p^{4.64}$
	$^2A_1$	1.52	0.11	-0.37	$[Rn]7s^{0.32}6d^{2.04}5f^{0.18}$	$[He]2s^{1.33}2p^{2.52}$	$[He]2s^{1.69}2p^{4.64}$
$Th^+(CO)_2$ ($D_{\infty h}$)	$^4\Sigma_g^-$	1.18	0.25	-0.34	$[Rn]7s^{0.85}6d^{1.89}5f^{0.07}$	$[He]2s^{1.42}2p^{2.29}$	$[He]2s^{1.70}2p^{4.60}$
	$^2\Sigma_g^-$	1.20	0.23	-0.34	$[Rn]7s^{0.83}6d^{1.88}5f^{0.07}$	$[He]2s^{1.42}2p^{2.30}$	$[He]2s^{1.70}2p^{4.60}$
$Th^+(CO)_2$ ($C_{\infty v}$) [a]	$^4\Delta$	1.25	0.18, 0.27	-0.35, -0.35	$[Rn]7s^{0.07}6d^{2.57}5f^{0.08}$	$[He]2s^{1.44,1.46}2p^{2.34,2.23}$	$[He]2s^{1.70}2p^{4.62}$
	$^2\Pi_g$	1.52	0.11	-0.37	$[Rn]7s^{0.07}6d^{2.30}5f^{0.10}$	$[He]2s^{1.42}2p^{2.43}$	$[He]2s^{1.70}2p^{4.64}$
	$^4\Pi_u$	1.70	0.03	-0.37	$[Rn]7s^{0.07}6d^{1.51}5f^{0.65}$	$He]2s^{1.44}2p^{2.50}$	$[He]2s^{1.70}2p^{4.64}$
$Th^+(CO)_2$ ($C_{\infty v}$) [a]	$^2\Delta$	1.28	0.20, 0.22	-0.35, -0.35	$[Rn]7s^{0.07}6d^{2.57}5f^{0.06}$	$[He]2s^{1.44,1.45}2p^{2.32,2.29}$	$[He]2s^{1.70}2p^{4.61}$
	$^2\Pi_u$	1.70	0.03	-0.38	$[Rn]7s^{0.07}6d^{1.49}5f^{0.67}$	$[He]2s^{1.44}2p^{2.50}$	$[He]2s^{1.70}2p^{4.64}$

[a] Symmetry-broken states (as discussed in the text).

Table S4. Energies and zero-point energies for stationary states calculated along the potential energy profiles of $Th^+C_2O_2$ for the formation of OTh^+CCO from addition of CO to $Th^+/Th^+(CO)$ calculated at the B3LYP/cc-pVQZ level[a]

Species (state)	Energy (E_h)	ZPE (E_h)[b]	E_{rel} (eV)[c]
$ThCO^+ + CO$ ($^4\Sigma^- + {}^1\Sigma^+$)	-633.284108	0.011680	0.00
$ThCO^+ + CO$ ($^2\Sigma^- + {}^1\Sigma^+$)	*-633.277379*	*0.011671*	*0.18*
$Th^+ + 2CO$ ($^4F + {}^1\Sigma^+$)	-633.226603	0.010090	1.52
$Th^+ + 2CO$ ($^2D + {}^1\Sigma^+$)	*-633.229957*	*0.010090*	*1.43*
1 $Th^+(CO)_2$ ($^4\Sigma_g^-$)	-633.313339	0.012910	-0.76
1 $Th^+(CO)_2$ ($^2\Sigma_g^-$)	*-633.307093*	*0.013095*	*-0.59*
TS1/2 (^{4}A")	-633.309577	0.012328 (149i)	-0.68
TS1/2 *(^{2}A')*	*-633.288269*	*0.012377 (169i)*	*-0.09*
2 $Th^+(CO)_2$ ($^4B_2$)	-633.327301	0.013368	-1.13
2 $Th^+(CO)_2$ ($^2B_1$)	*-633.320812*	*0.014015*	*-0.94*
TS2/3 (^{4}A)	-633.295005	0.011814 (279i)	0.29
TS2/3 (^{2}A)	*-633.290028*	*0.011844 (281i)*	*0.16*
3 $OCTh^+(\eta^2–CO)$ (^{4}A)	-633.303217	0.012275	-0.50
3 $OCTh^+(\eta^2–CO)$ (^{2}A)	*-633.296719*	*0.012231*	*-0.33*
^{4}TS3/4 (^{4}A)	-633.297915	0.011797 (126i)	-0.37
^{4}4 $Th^+(\eta^3–OC(CO))$ (^{4}A")	-633.300014	0.0124626	-0.41
^{4}TS4/5 (4A")	-633.274621	0.012179 (393i)	0.27
^{4}5 $Th^+(\eta^3–OCCO)$ (^{4}A")	-633.276543	0.012990	0.24

Table S3. Contd.

^{4}TS5/6 (^{4}A")	-633.269163	0.014296 (249i)	0.48
^{2}TS3/6 (^{2}A)	*-633.271599*	*0.011076 (610i)*	*0.32*
6 $Th^+(\eta^2$–OCCO) (^{4}A")	-633.296632	0.015393	-0.24
6 $Th^+(\eta^2$–OCCO) (^{2}A')	*-633.347456*	*0.015547*	*-1.62*
TS6/7 (^{4}A")	-633.271981	0.012480 (739i)	0.35
TS6/7 (^{2}A')	*-633.330979*	*0.013536 (1042i)*	*-1.22*
7 OTh^+CCO (^{4}A")	-633.3115412	0.0128411	-0.71
7 OTh^+CCO (^{2}A')	*-633.4005755*	*0.0139323*	*-3.11*

[a] Values for quartet and doublet species are indicated in roman and italics font, respectively.

[b] Zero-point energy. Imaginary frequencies in cm^{-1} are included in parentheses.

[c] Energies are relative to $Th^+(CO)$ ($^4\Sigma^-$) + CO ($^1\Sigma^+$). No spin-orbit corrections are included.

Table S5. Energies and zero-point energies for optimized structures calculated using different levels of theory [a]

Species (state)	Basis Sets	Level of Theory	Energy (E_h)	ZPE (E_h)	$<s^2>$
CO ($^1\Sigma^+$, $C_{\infty v}$)	SDD	B3LYP	-113.35679	0.005051	0.00
		BHLYP	-113.299148	0.005304	0.00
		MP2	-113.136471	0.005051	0.00
		CCSD(T)	-113.156536	0.005051	0.00
	cc-pVTZ	B3LYP	-113.358513	0.005032	0.00
		BHLYP	-113.300378	0.005286	0.00
		MP2	-113.139229	0.005032	0.00
		CCSD(T)	-113.159112	0.005032	0.00
	cc-pVQZ	B3LYP	-113.366764	0.005045	0.00
		BHLYP	-113.308749	0.005299	0.00
		MP2	-113.169644	0.005045	0.00
		CCSD(T)	-113.187776	0.005045	0.00
	CBS	B3LYP	-113.369023	0.005045	
		BHLYP	-113.311041	0.005299	
		MP2	-113.184644	0.005045	
		CCSD(T)	-113.201765	0.005045	
CCO ($^3\Sigma^-$, $C_{\infty v}$)	cc-pVQZ	B3LYP	-151.328379	0.008884	2.01
$ThCO^+$ ($^4\Sigma^-$, $C_{\infty v}$)	SDD	B3LYP	-520.737507	0.006677	3.75
		BHLYP	-520.439647	0.006949	3.76
		MP2	-519.055811	0.006677	3.79
		CCSD(T)	-519.082853	0.006677	3.79
	cc-pVTZ	B3LYP	-519.908720	0.006639	3.75
		BHLYP	-519.600176	0.006912	3.76
		MP2	-518.211641	0.006639	3.80
		CCSD(T)	-518.238247	0.006639	3.80
	cc-pVQZ	B3LYP	-519.917316	0.006640	3.75
		BHLYP	-519.608788	0.006914	3.76
		MP2	-518.244039	0.006640	3.79
		CCSD(T)	-518.268881	0.006640	3.79
	CBS	B3LYP	-519.919669	0.006640	
		BHLYP	-519.611146	0.006914	
		MP2	-518.260127	0.006640	
		CCSD(T)	-518.283951	0.006640	

Table S5. continued.

Species (state)	Basis Sets	Level of Theory	Energy (E_h)	ZPE (E_h)	$<s^2>$
$Th(CO)_2^+$ ($^4B_2$, C_{2v})	SDD	B3LYP	-634.136407	0.013442	3.76
		BHLYP	-633.774907	0.014031	3.76
		MP2	-632.228136	0.013442	3.81
		CCSD(T)	-632.271533	0.013442	3.81
	cc-pVTZ	B3LYP	-633.310857	0.013353	3.76
		BHLYP	-632.938011	0.013949	3.76
		MP2	-631.389120	0.013353	3.81
		CCSD(T)	-631.431857	0.013353	3.81
	cc-pVQZ	B3LYP	-633.327301	0.013368	3.76
		BHLYP	-632.954656	0.013965	3.76
		MP2	-631.452689	0.013368	3.81
		CCSD(T)	-631.492080	0.013368	3.81
	CBS	B3LYP	-633.331803	0.013368	
		BHLYP	-632.959214	0.013965	
		MP2	-631.484232	0.013368	
		CCSD(T)	-631.521692	0.013368	
$Th(CO)_2^+$ ($^4B_1$, C_{2v})	cc-pVQZ	B3LYP	-633.322359	0.013552	3.75
$Th(CO)_2^+$ ($^2B_1$, C_{2v})			-633.320812	0.014015	0.76
$Th(CO)_2^+$ ($^2A_1$, C_{2v})			-633.316527	0.014158	0.77
$Th(CO)_2^+$ ($^4B_1$, C_{2v})			-633.313423	0.013053	3.75
$Th(CO)_2^+$ ($^4\Sigma_g^-$, $D_{\infty h}$)			-633.313339	0.012910	3.75
$Th(CO)_2^+$ ($^2\Sigma_g^-$, $D_{\infty h}$)			-633.307093	0.013093	1.75
$Th(CO)_2^+$ ($^4\Delta$, $C_{\infty v}$)			-633.296676	0.013741	3.75
$Th(CO)_2^+$ ($^2\Pi_g$, $D_{\infty h}$)			-633.296058	0.013685	0.75
$Th(CO)_2^+$ ($^4\Pi_u$, $D_{\infty h}$)			-633.292883	0.013626	3.76
$Th(CO)_2^+$ ($^2\Delta$, $C_{\infty v}$)			-633.286424	0.013747	1.75
$Th(CO)_2^+$ ($^2\Pi_u$, $D_{\infty h}$)			-633.286474	0.013861	1.76
OTh^+CCO (^{2}A', Cs)	cc-pVTZ	B3LYP	-633.384640	0.013968	0.76
		BHLYP	-633.006613	0.014553	0.77
	cc-pVQZ	B3LYP	-633.400576	0.013932	0.76
		BHLYP	-633.022871	0.014513	0.77
OTh^+CCO (^{4}A", Cs)	cc-pVTZ	B3LYP	-633.295232	0.012862	3.77
		BHLYP	-632.923139	0.013536	3.78
	cc-pVQZ	B3LYP	-633.311541	0.012841	3.77
ThO^+ ($^2\Sigma^+$, $C_{\infty v}$)	cc-pVQZ	B3LYP	-481.931217	0.002198	0.75

[a] All theoretical values from structures optimized at the respective level of theory with the indicated basis set, except MP2 and CCSD(T), which are single point energy calculations using the B3LYP optimized structures with the indicated basis set.

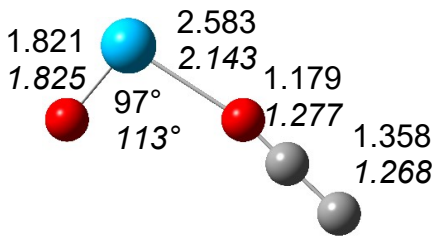

OTh⁺OCC (^{4}A" *(^{2}A')*, C_s)
1.34 *(-0.12)*

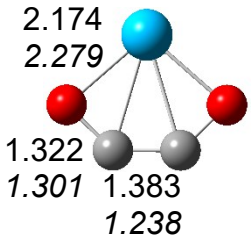

Th⁺(η⁴–OCCO) (^{4}A$_2$,365i *(^{2}A$_1$)*, C_{2V})
1.66 *(0.22)*

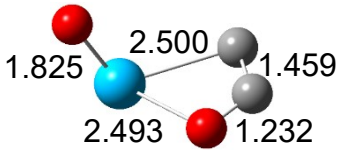

OTh⁺(η²–OC(C)) (^{4}A, C_1)
0.65

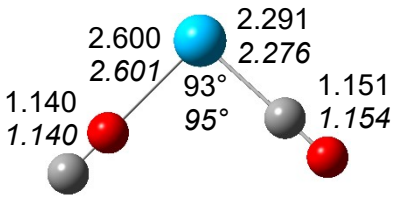

COTh⁺CO (^{4}A" *(^{2}A")*, C_s)
0.75 *(0.94)*

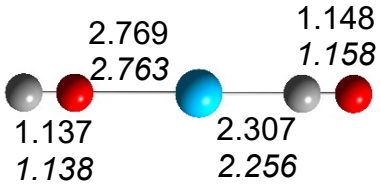

COTh⁺CO ($^4\Sigma^-$ *($^2\Pi$)*, $C_{\infty v}$)
0.78 *(1.75)*

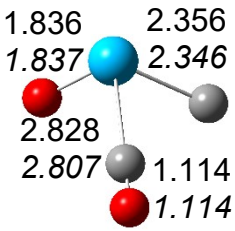

Th⁺(η³–OC(CO)) (^{4}A *(^{2}A)*, C_1)
0.79 *(1.31)*

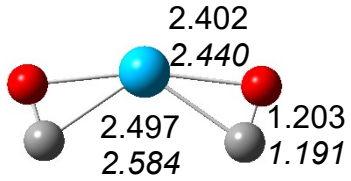

Th⁺(η³–OC(CO)) (^{4}A *(^{2}A)*, C_1)
1.37 *(1.77)*

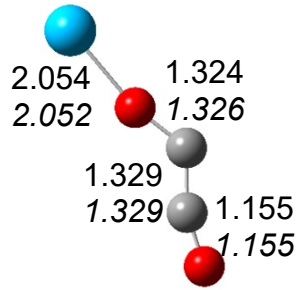

Th⁺OCCO (^{4}A" *(^{2}A')*, C_s)
1.46 *(1.48)*

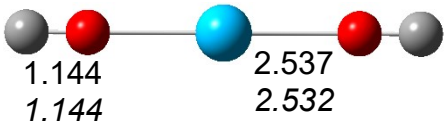

Th⁺(OC)$_2$ ($^4\Sigma_g^-$ *($^2\Pi$)*, $C_{\infty v}$)
1.98 *(1.74)*

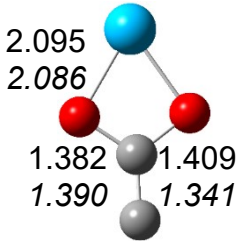

Th⁺(η²–OO(CC)) (^{4}A$_2$,91i *(^{2}A$_1$)*, C_{2V})
2.30 *(1.55)*

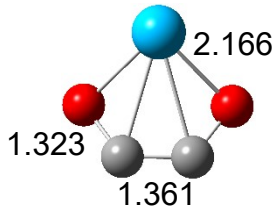

Th⁺(η⁴–OCCO) (^{4}A", C_S)
1.22

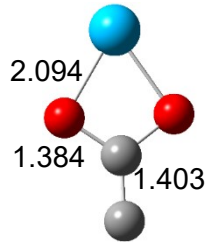

Th⁺(η²–OO(CC)) (^{4}A", C_S)
2.31

Figure S1. Structures of different isomers of $[Th,2C,2O]^+$ and their relative energies in eV with respect to the $Th^+(CO)_2$ ($^4B_2$) state calculated at the B3LYP/cc-pVQZ level. Selected bond lengths (Å) and bond angles (°) are indicated, quartet in roman font and doublet in *italics font*. Some isomers that are spin sensitive and not stable in a particular point group are indicated by their imaginary frequency (i) in cm^{-1}. Th – blue, C – grey, O – red. None of these isomers are involved in the rearrangement pathways of $Th^+(CO)_2$ to OTh^+CCO, and as such, they are not included in Figures 4 and 5 of the main text.

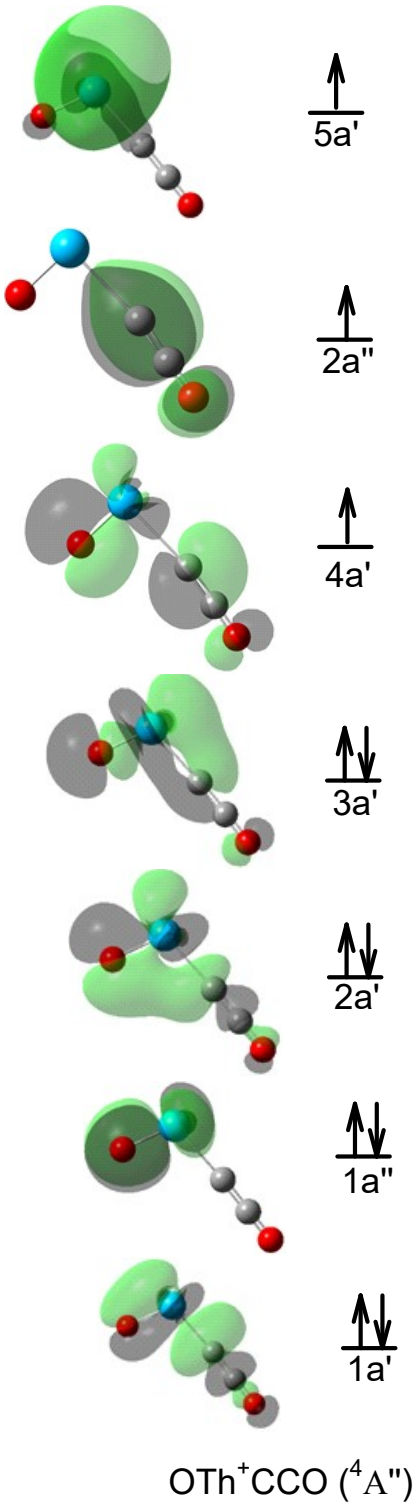

Figure S2. Valence electronic configurations and molecular orbitals for quartet cationic thorium oxide ketenylidene, $OTh^{+}CCO$ ($^{4}A"$), as calculated at the B3LYP/cc-pVQZ level. Th – blue, C – grey, O – red.